

An Effective MIMO Antenna Design for 5G Communication

J.Jaya Keerthana¹, S.Kiran Mohana Rao², V.Sri Vidya³, P.Aravin⁴, M.Dora Swamy Bhagya Raju⁵

¹ Assistant Professor, Dept. of Electronics and Communication Engineering Department, Seshadri Rao Gudlavalleru Engineering College, Andhra Pradesh, India

^{2,3,4,5} Student, Department of Electronics and Communication Engineering, Seshadri Rao Gudlavalleru Engineering college, Andhra Pradesh, India

Abstract- Industry 5.0 emphasizes the development of highly connected, intelligent, and sustainable communication ecosystems, where advanced 5G and emerging 6G technologies play a crucial role. Antennas serve as fundamental components in enabling these high-speed wireless networks, necessitating compact, wideband, and high-efficiency designs. In this work, a compact Rectangular microstrip antenna with hexagonal slots is designed and modelled for ultra-wideband (UWB) applications with a specific focus on 5G mobile communication systems. The hexagonal geometry is selected over conventional rectangular and circular patches due to its inherent advantages, including improved harmonic suppression, scalable bandwidth, and symmetric radiation characteristics, which contribute to reduced cross-polarization and enhanced multi-band performance. The proposed antenna is designed on a low-cost FR-4 substrate with a compact footprint of 30 mm × 30 mm and is optimized to achieve wide impedance bandwidth and stable radiation performance. To further enhance system reliability and channel capacity, the design is extended into a Multiple-Input Multiple-Output (MIMO) configuration. Key MIMO performance metrics such as S-parameters, Envelope Correlation Coefficient (ECC), and diversity gain, Mean Effective Gain (MEG) are analysed and modelled using CST Microwave Studio and Google colab. A comparative evaluation with recent antenna designs demonstrates that the proposed MIMO antenna offers superior performance in terms of bandwidth, gain, compactness, and radiation efficiency. Owing to its compact structure, wideband characteristics, and improved MIMO performance, the proposed antenna is a promising candidate for next-generation 5G and future 6G wireless communication and Industry 5.0 applications.

Keywords—antenna, Multiple-Input Multiple-Output (MIMO), Ultra-Wideband, Hexagonal Patch, FR-4 Substrate, Envelope Correlation Coefficient, Diversity Gain, 5G Communication.

1 INTRODUCTION

The rapid advancement of wireless communication technologies has significantly increased the demand for high data rates, improved spectral efficiency, and enhanced link reliability. With the deployment of fifth-generation (5G) and the ongoing research toward sixth-generation (6G) systems, modern wireless networks must

support massive connectivity, ultra-low latency, and high throughput. One of the key technologies enabling these requirements is Multiple-Input Multiple-Output (MIMO) antenna systems.

MIMO technology employs multiple transmitting and receiving antennas to exploit spatial diversity and multipath propagation, thereby increasing channel capacity without requiring additional bandwidth or transmit power. Compared to conventional single-input single-output (SISO) systems, MIMO systems provide substantial improvements in data rate, signal reliability, and spectral efficiency. This makes MIMO an essential component in 4G LTE, 5G NR, wireless local area networks (WLAN), Internet of Things (IoT) devices, and future smart communication infrastructures.

MIMO technology employs multiple transmitting and receiving antennas to exploit multipath propagation effectively. Instead of treating multipath signals as interference, MIMO systems utilize them to improve signal strength and data throughput. The performance improvement is achieved through diversity gain and spatial multiplexing techniques. The theoretical diversity order of a MIMO system is given by the product of the number of transmit and receive antennas ($N_t \times N_r$), which significantly enhances system robustness against fading.

Microstrip patch antennas are widely used in MIMO configurations due to their low profile, lightweight structure, low fabrication cost, and compatibility with printed circuit board technology. However, designing compact MIMO antennas for Ultra-Wideband (UWB) and 5G applications presents challenges such as mutual coupling between antenna elements, high envelope correlation coefficient (ECC), and reduced isolation. Therefore, proper design techniques such as defected ground structures (DGS), orthogonal element placement, and neutralization lines are adopted to improve isolation and overall MIMO performance.

In this work, a compact MIMO antenna is designed and analysed to achieve wide impedance bandwidth, high isolation, low ECC, and stable radiation characteristics. The proposed design aims to provide enhanced diversity performance and improved spectral efficiency, making it suitable for next-generation 5G and future 6G wireless communication applications.

2 DESIGN OF SINGLE HEXAGON ANTENNA

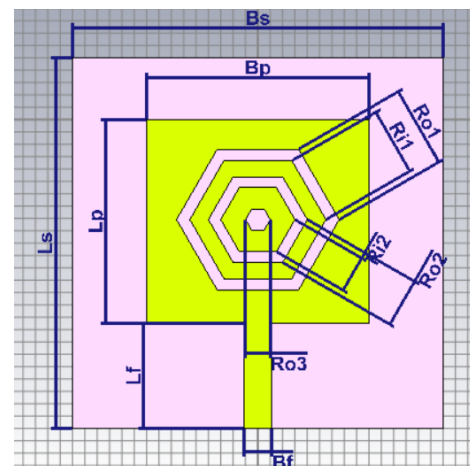
Ultra-wideband technology, which also enables users to wirelessly link a large number of devices and a large number of users in the areas of dispatch and reception, eliminates the need for cables for users of wireless systems.

The design of the proposed single Rectangular microstrip patch antenna with hexagonal slots is carried out to achieve compact size, wide impedance bandwidth, and stable radiation performance suitable for modern wireless communication applications. The hexagonal geometry is selected instead of conventional rectangular or circular shapes due to its symmetrical structure, improved current distribution, and better harmonic suppression characteristics. The symmetrical configuration of the hexagon helps in achieving balanced radiation patterns and reduced cross-polarization levels.

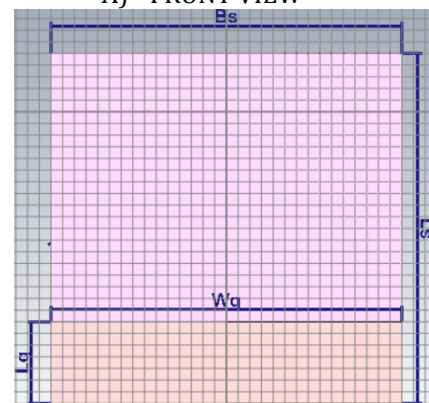
The antenna is fabricated on an FR-4 dielectric substrate with an appropriate of 1.6mm thickness and dielectric constant 4.4 to maintain a balance between bandwidth, efficiency, and fabrication cost. A copper layer is used for both the radiating patch and the ground plane. The side length of the hexagonal patch is carefully optimized to resonate at the desired operating frequency of 3.75GHz. The resonant frequency primarily depends on the effective radius (or equivalent dimension) of the hexagon, substrate permittivity, and thickness.

To enhance impedance matching and bandwidth performance, a microstrip feed line is employed. The feed position is optimized to achieve minimum return loss (S11) at the operating frequency. Proper impedance matching ensures efficient power transfer between the transmission line and the radiating patch. The antenna design parameters are modelled and simulated using CST Microwave Studio to analyse return loss, Voltage Standing Wave Ratio (VSWR), gain, and radiation pattern characteristics.

The optimized single antenna serves as the fundamental radiating element for further extension into a MIMO configuration. Its compact structure, stable radiation characteristics, and wideband response make it suitable for integration into advanced 5G and Ultra-Wideband (UWB) communication systems.



A) FRONT VIEW



B) BACK VIEW

Figure1: Single Rectangular patch with hexagonal slotted antenna.

The proposed antenna is designed on a square dielectric substrate with overall dimensions $L_s \times B_s = 30 \text{ mm} \times 30 \text{ mm}$, where L_s represents the length of the substrate and B_s represents the width of the substrate. The radiating patch is placed at the center of the substrate with dimensions $L_p \times B_p = 16.5 \text{ mm} \times 18 \text{ mm}$. The antenna is excited using a microstrip feed line having a length (L_f) of 8.5 mm and width (B_f) of 2.30 mm, ensuring proper impedance matching. To enhance the antenna performance, concentric hexagonal slots are etched in the patch, where the outer hexagonal radius (R_{o1}) is 5.50 mm and the inner hexagonal radius (R_{i1}) is 4.00 mm. The spacing between the slots is maintained at 2.00 mm, which increases the effective current path length and improves the impedance bandwidth and radiation characteristics of the antenna.

Inside the patch, concentric hexagonal slots are introduced to enhance the current distribution and improve the antenna performance. The outer and inner hexagonal slot radii are 5.50 mm and 4.00 mm, respectively. The spacing between the slots is maintained at 2.00 mm, which helps in increasing the effective current path length. This

modification improves the impedance bandwidth and radiation characteristics of the antenna.

The compact geometry, along with the slotted hexagonal structure and microstrip feed, enables the antenna to achieve improved bandwidth, good impedance matching, and stable radiation performance, making it suitable for wideband wireless communication applications.

Table-1: PROPOSED ANTENNA DIMENSION VALUES

Parameter	Length (mm)	Width (mm)	Height (mm)
Ground	7	30	0.035
Substate	27	22	1.6
Patch	15.5	16	1.6
Feed	18.6	2.3	1.6

2.1 Design equations of a Microstrip patch antenna

The resonant frequency of a microstrip patch antenna primarily depends on the physical dimensions of the radiating element and the dielectric properties of the substrate.

The width of the microstrip patch can be determined using

$$W = \frac{c}{2f_r} \sqrt{\frac{2}{\epsilon_r + 1}} \quad (1)$$

The effective relative dielectric constant plays a significant role in determining the resonant length. It can be calculated as:

$$\epsilon_{eff} = \frac{\epsilon_r + 1}{2} + \frac{\epsilon_r - 1}{2} \left(1 + 12 \frac{h}{W}\right)^{-1/2} \quad (2)$$

where ϵ_r is the dielectric constant of the substrate, h is the substrate thickness, and W is the width of the patch.

The effective length (L_{eff}) of the patch is given by:

$$L_{eff} = \frac{c}{2f_r \sqrt{\epsilon_{eff}}} \quad (3)$$

where c is the speed of light and f_r is the resonant frequency. The actual physical length (L) of the patch is then obtained by subtracting the fringing field extension from the effective length.

Due to fringing fields at the patch edges, the physical length of the antenna becomes slightly smaller than the effective length. The length extension (ΔL) caused by fringing fields can be calculated as

$$\Delta L = 0.412h \frac{(\epsilon_{eff} + 0.3) \left(\frac{W}{h} + 0.264\right)}{(\epsilon_{eff} - 0.258) \left(\frac{W}{h} + 0.8\right)} \quad (4)$$

Thus, the actual length of the patch antenna is

$$L = L_{eff} - 2\Delta L \quad (5)$$

The design calculations of the proposed antenna are performed using the fundamental parameters of the strate and operating frequency.

The resonant frequency (f_r) of the antenna is selected as 3.75 GHz. The antenna is fabricated on an FR4 substrate with a dielectric constant of 4.4 and a substrate thickness (h) of 1.6 mm. The speed of light in free space (c) is taken as (3×10^8) m/s, which is used in determining the patch dimensions and resonant characteristics of the antenna. These parameters are utilized in the standard microstrip antenna design equations to calculate the effective dielectric constant, patch width, and effective length of the antenna.

1. Width of the Patch

$$W = \frac{c}{2f_r} \sqrt{\frac{2}{\epsilon_r + 1}}$$

$$W = \frac{3 \times 10^8}{2 \times 3.75 \times 10^9} \sqrt{\frac{2}{5.4}}$$

$$W = 0.0243 \text{ m} \approx 24.34 \text{ mm}$$

2. Effective Dielectric Constant ϵ_{eff}

$$\epsilon_{eff} = \frac{\epsilon_r + 1}{2} + \frac{\epsilon_r - 1}{2} \left(1 + 12 \frac{h}{W}\right)^{-1/2}$$

$$\epsilon_{eff} = 2.7 + 1.7(1 + 0.788)^{-1/2}$$

$$\epsilon_{eff} \approx 3.97$$

3. Effective Length L_{eff}

$$L_{eff} = \frac{c}{2f_r \sqrt{\epsilon_{eff}}}$$

$$L_{eff} = \frac{3 \times 10^8}{2 \times 3.75 \times 10^9 \sqrt{3.97}}$$

$$L_{eff} \approx 20.07 \text{ mm}$$

4. Fringing Length Extension ΔL

$$\Delta L = 0.412h \frac{(\epsilon_{eff} + 0.3)(W/h + 0.264)}{(\epsilon_{eff} - 0.258)(W/h + 0.8)}$$

$$\Delta L \approx 0.73 \text{ mm}$$

5. Actual Patch Length L

$$L = L_{eff} - 2\Delta L$$

$$L = 20.07 - 1.46$$

$$L \approx 18.6 \text{ mm}$$

These analytical equations provide the initial design dimensions of the antenna. The final dimensions are further optimized to achieve the required dual-band performance, improved return loss, and enhanced radiation efficiency.

2.2 Evolution stages of Design of Microstrip Patch Antenna

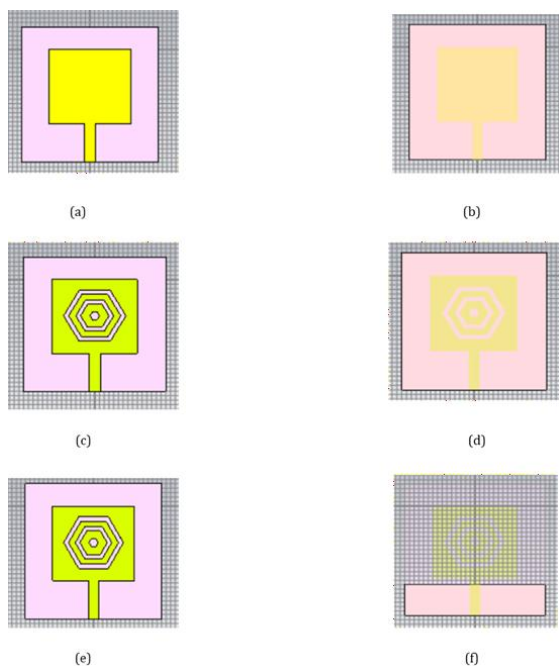


Figure2: Evolution stages of Design of Microstrip Patch Antenna.

The figure illustrates the step-by-step design evolution of the proposed microstrip patch antenna. Initially, a basic rectangular microstrip patch with a microstrip feed line is designed on the substrate to obtain the fundamental resonant characteristics. In the second stage, hexagonal slot structures are introduced on the radiating patch, which modify the surface current distribution and help in improving the bandwidth and impedance matching. Further optimization is performed by adjusting the slot

geometry and patch structure to achieve better radiation performance. Finally, the complete optimized antenna structure along with the ground plane configuration is obtained, which enhances the overall antenna characteristics such as gain, bandwidth, and return loss, making the antenna suitable for the desired 3-5 GHz wireless communication applications.

Table -2: Characteristics of the developed antenna with Partial Ground at various steps

Type of antenna design structure	Resonant frequency (GHz)	Return loss (dB)	VSWR	Bandwidth (MHz)
Rectangular Microstrip patch antenna with full Ground	4.1	-6.8	2.7	300
Rectangular Microstrip patch antenna with hexagonal slots and full Ground	3.3	-3.7	4.9	800
Rectangular Microstrip patch antenna with hexagonal slots and Partial Ground	3.75	-50	1.1	2200

2.3 Results of microstrip patch

The performance of the designed microstrip patch antenna is evaluated using S-parameters and Voltage Standing Wave Ratio (VSWR).

2.3.1 S-parameter

Scattering parameters, commonly known as S-parameters, are widely used to analyse the performance of antennas and high-frequency microwave circuits. They describe

how radio frequency (RF) signals behave when they encounter a network, particularly how much power is reflected, transmitted, or coupled between different ports of the antenna system.

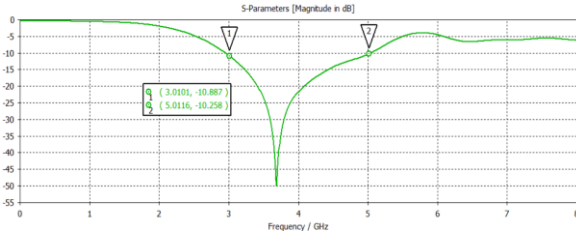


Figure3: S-parameters of the proposed Microstrip patch antenna.

The S-parameter (S11) plot shows the reflection coefficient of the proposed antenna over the frequency range. From the graph, a deep resonance occurs around 3.7 GHz, where the return loss reaches approximately -48 dB, indicating excellent impedance matching and very low signal reflection. Additional points are observed at 3.0 GHz and 5.0 GHz, where the return loss values are about -10.87 dB and -10.35 dB, respectively, which are below the -10 dB threshold and therefore considered acceptable for antenna operation. This indicates that the antenna provides good impedance matching and operates efficiently within the 3–5 GHz frequency band.

2.3.2 VSWR

Voltage Standing Wave Ratio (VSWR) is an important parameter used to evaluate the impedance matching between the antenna and the transmission line. For efficient antenna operation, the VSWR value should ideally be close to 1 and typically less than 2 within the operating frequency band.

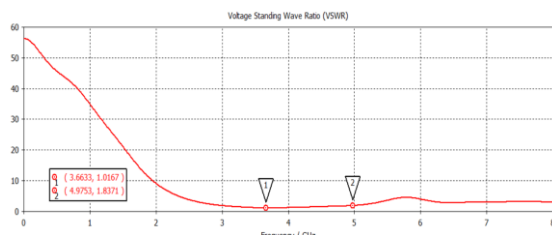


Figure 4: VSWR of the proposed Microstrip patch antenna.

From the graph, the antenna exhibits a minimum VSWR of approximately 1.11 at around 3.7GHz, indicating excellent impedance matching at the resonant frequency. Another point is observed at 4.98 GHz with a VSWR value of about 1.84, which is still within the acceptable limit of $VSWR < 2$ for efficient antenna operation. The VSWR remains close to unity in the 3–5 GHz frequency range, confirming that the antenna provides good impedance matching and minimal power reflection in this band. This demonstrates that the antenna is suitable for mid-band wireless

communication applications, offering stable performance and efficient radiation characteristics within the operating band.

3 PARAMETRIC ANALYSES OF RECTANGULAR PATCH ANTENNA WITH HEXAGONAL SLOTS

This section provides a parametric analysis of a hexagon UWB antenna. The degree bandwidth and radiation designs of these setups have been assessed to make sure they are compatible with the expected results.

3.1 The Effect of Patch Length (Lp) on Antenna Performance

Patch-length (Lp) is another important design parameter for setting an appropriate resonant frequency of the antenna. An increase in Lp increases the electrical length of the antenna, which in turn reduces the resonant frequency all the way to Lp. Decreasing it will make Lp resonate at higher frequencies.

In our simulations, a reduced Lp resulted in degradation in impedance matching, thereby resulting in a weak signal and bandwidth. After experimenting with various values, an Lp value of 16.5 mm achieved the best compromise to give a resonant frequency of 3.75 GHz with excellent return loss $S_{11} = -50\text{dB}$.

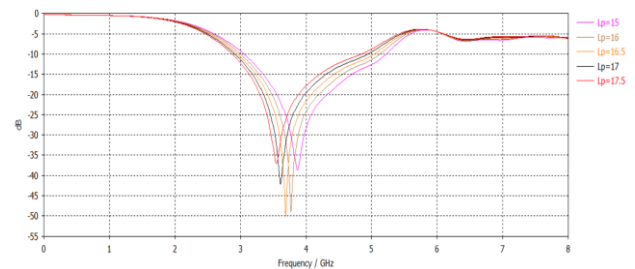


Figure5: Parametric analysis of developed antenna Patch length (Lp)

3.2 Effect of Ground Length (Lg) on Antenna Performance

The length of ground (Lg) is an important consideration that affects the bandwidth and radiation efficiency. A larger Lg will shift the resonant frequency lower, although it may narrow the bandwidth and thus affect the overall antenna performance. On the other hand, an excessively small Lg may cause impedance mismatches, resulting in high S11 values and losses in efficiency. The best overall tuning was achieved at $L_g = 34.5\text{mm}$ in that 4.9 GHz bandwidth was maintained at decent antenna performance with stable radiation patterns.

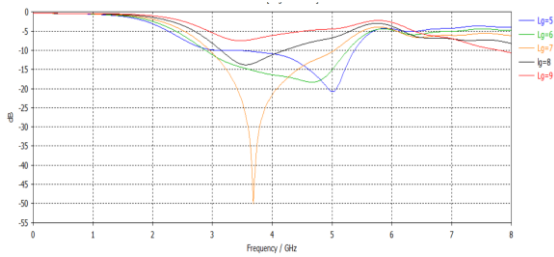


Figure 6: Parametric analysis of developed antenna Ground length (Lg)

3.3 Effect of Patch Width (Wp) on Antenna Performance

The patch width (Wp) takes an important role in shaping the input impedance and surface current distributions. Wider patches generally improve gain and radiation efficiency; however, if the patch becomes too wide, unwanted resonances may result which affect impedance matching. Tests showed that S11 values improved as Wp increased until a certain limit was obtained, beyond which variations in gain occurred. Wp = 18 mm appears ideally balanced, giving a return loss of -50 dB.

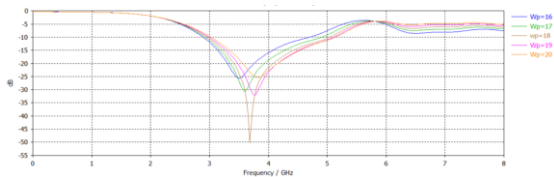


Figure 7: Parametric analysis of developed antenna Patch width (Wp)

3.4 The Length of Substrate (Ls) and its Influence on Antenna Performance

The substrate length (Ls) dictates the mode of wave propagation in the antenna and has an influence on bandwidth and impedance stability. A bigger Ls means that the substrate is a good supporter for surface wave propagation, but with an increase in microwave dielectric losses. Ls must not be too small because in this way, it will limit current flow and eventually affect impedance matching and bandwidth. Through trial and error, an optimum Ls of 32 mm showed to provide an efficient performance with broadband response and stable impedance characteristics subject to minimum losses.

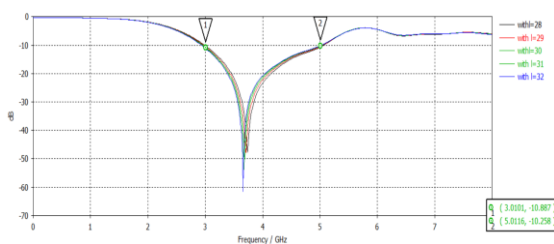
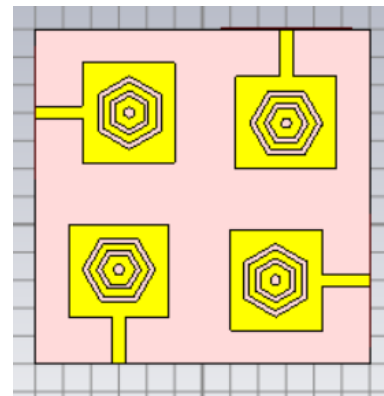


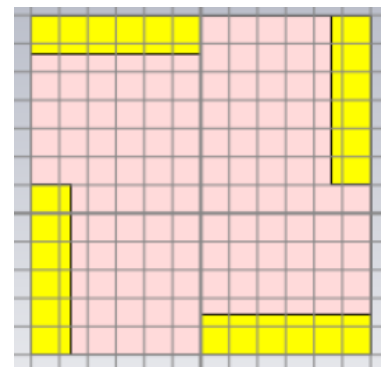
Figure 8: Parametric analysis of developed antenna Length of Substrate.

4.4.4 MIMO ANTENNA MODEL

The suggested antenna is made up of four individual antenna components arranged in orthogonal orientations to create a MIMO prototype. The four identical antenna components are assembled into a Printed Circuit Board (PCB), which has three layers of patch, ground, and dielectric substrate. The same components are utilized for the single element that is suggested and has the dimensions 60 × 60 * 1.6mm3 in Fig. 6.



A) FRONT VIEW



B) BACK VIEW

Figure 9: The MIMO antenna

5 MIMO ANTENNA PARAMETERS

To evaluate the performance of MIMO antennas, several important parameters are analysed, including Envelope Correlation Coefficient (ECC), Diversity Gain (DG), Mean Effective Gain (MEG), Channel Capacity Loss (CCL), and Total Active Reflection Coefficient (TARC).

5.1 Envelope Correlation Coefficient (ECC)

Envelope Correlation Coefficient (ECC) is an important parameter in MIMO antenna systems that measures the correlation between radiation patterns of different antenna elements. It indicates how independently the antennas operate from each other. In a good MIMO system, each antenna should transmit and receive signals independently to achieve high diversity and improved channel capacity. ECC values range from 0 to 1.

For practical MIMO antennas, ECC should be less than 0.5, and for high-performance systems, it is preferably less than 0.05. Lower ECC results in better diversity gain, improved signal reliability, and higher data throughput in wireless communication systems.

$$\rho_e(i, j, N) = \frac{|\sum_{n=1}^N S_{in}^* S_{nj}|^2}{\prod_{k=i,j} [1 - \sum_{n=1}^N S_{kn}^* S_{nk}]} \quad (6)$$

The above equation depicts the envelope correlation between the antennas i and j in the (N,N) MIMO system. In case of $i= 1, j=2$ and $N=4$, the envelope correlation of proposed MIMO antenna can be defined as follows

$$\begin{aligned} \rho_e(1,2,4) &= |S_{11}^* S_{12} + S_{12}^* S_{22} + S_{13}^* S_{32} + S_{14}^* S_{42}|^2 \\ &\times ([1 - (S_{11}^* S_{11} + S_{12}^* S_{21} + S_{13}^* S_{31} + S_{14}^* S_{41})] \\ &\times [1 - (S_{11}^* S_{12} + S_{12}^* S_{22} + S_{13}^* S_{32} + S_{14}^* S_{42})])^{-1}. \end{aligned}$$

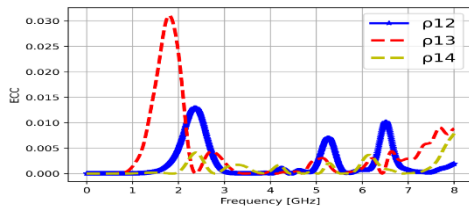


Figure 10: Envelope Correlation Coefficient (ECC)

The Envelope Correlation Coefficient (ECC) of the proposed MIMO antenna remains very low across the operating frequency range, with peak values below 0.03. Such low ECC values (less than 0.05) indicate excellent isolation and minimal correlation between antenna elements. This confirms good diversity performance and effective MIMO operation over the UWB band.

5.2 Diversity Gain (DG)

Diversity Gain (DG) in a MIMO antenna system refers to the improvement in signal reliability achieved by using multiple antenna elements to combat multipath fading. DG is typically close to 10 dB, which indicates strong diversity performance and low correlation between antenna elements. A higher diversity gain means better signal stability, improved link quality, and enhanced overall communication reliability.

$$DG = 10\sqrt{1 - |ECC|^2} \quad (7)$$

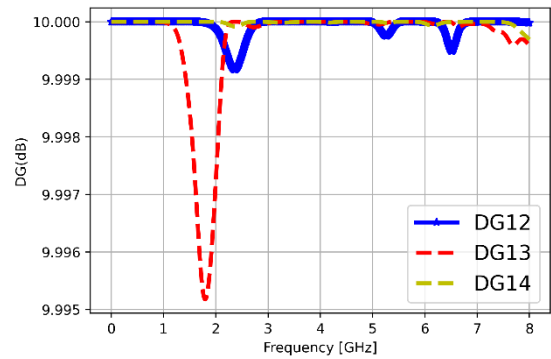


Figure 11: Diversity Gain (DG)

5.3 Mean Effective Gain (MEG)

Mean Effective Gain (MEG) is a MIMO antenna parameter that represents the average received power of an antenna element in a multipath propagation environment. It evaluates how effectively each antenna receives signals when waves arrive from different directions with varying polarizations. Ideally, the ratio of MEG between any two antenna elements should be close to 1 (or within ± 3 dB). Proper MEG balance helps achieve better diversity performance, improved signal quality, and higher channel capacity in MIMO communication systems.

$$MEG_i = \frac{1}{2} \left(1 - \sum_{j=1}^N |S_{ij}|^2 \right) \quad (8)$$

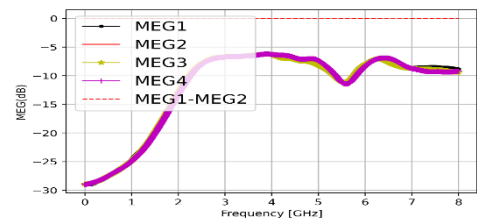


Figure 12: Mean Effective Gain (MEG)

The MEG curves of all four antenna elements are nearly identical across the operating band, indicating uniform radiation performance in the MIMO configuration. The difference between MEG1 and MEG2 remains close to 0 dB, satisfying the acceptable diversity condition ($|MEG1 - MEG2| < 3$ dB). This confirms balanced power distribution and good MIMO efficiency.

5.4 Total Active Reflection Coefficient (TARC)

Total Active Reflection Coefficient (TARC) measures the overall reflection performance when multiple antenna ports are excited simultaneously.

TARC is calculated using the reflected and incident voltage waves from all antenna ports, and for good MIMO performance, its value should generally be below **-10 dB** within the operating frequency band. A lower TARC

indicates better impedance matching, reduced mutual coupling, and improved overall efficiency of the MIMO antenna system.

$$TARC(\theta) = \sqrt{\frac{|\sum_{i=1}^N \sum_{j=1}^N S_{ij} e^{j\theta_j}|^2}{N}} \quad (9)$$

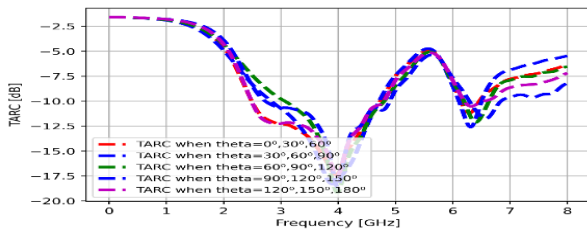


Figure 13: Total Active Reflection Coefficient

In the plot TARC remains below -10 dB over the main operating bands(3-5GHz) for different excitation phase angles, indicating good impedance matching in the MIMO configuration. The curves show consistent behavior across various theta combinations, demonstrating stable multi-port performance. This confirms efficient power radiation and reliable MIMO operation across the UWB frequency range.

5.5 Channel Capacity Loss (CCL)

Channel Capacity Loss (CCL) is a key performance parameter in MIMO antenna systems that quantifies the reduction in theoretical maximum data transmission capacity due to correlation and mutual coupling between antenna elements. CCL is calculated using S-parameters and reflects how much the real antenna deviates from ideal behavior. For good MIMO performance, the Channel Capacity Loss should typically be less than 0.4 bits/Hz within the operating frequency band. A lower CCL indicates better isolation, lower correlation, and higher data throughput capability.

$$CCL = -\log^2(\det(\Psi^R)) \quad (10)$$

$$\Psi^R = \begin{bmatrix} \rho_{11} & \rho_{12} & \rho_{13} & \rho_{14} \\ \rho_{21} & \rho_{22} & \rho_{23} & \rho_{24} \\ \rho_{31} & \rho_{32} & \rho_{33} & \rho_{34} \\ \rho_{41} & \rho_{42} & \rho_{43} & \rho_{44} \end{bmatrix}$$

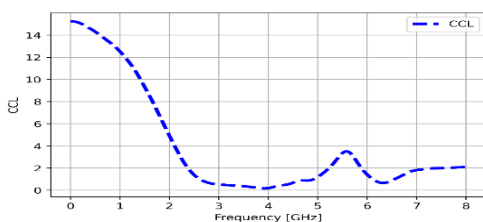


Figure14: Mean Effective Gain (MEG)

In the 3–5 GHz frequency range, the Channel Capacity Loss (CCL) remains very low, approximately close to 0–0.5 bits/s/Hz. This indicates minimal loss in channel capacity and low correlation between the antenna elements. Hence, the MIMO antenna exhibits efficient diversity performance and reliable operation within this band.

6 CONCLUSION

In this work, a compact rectangular microstrip patch antenna with hexagonal slots has been designed and analysed for ultra-wideband wireless communication applications. The antenna is simulated on an FR-4 substrate with compact dimensions of 30 mm × 30 mm and operates within the 3–5 GHz frequency band, making it suitable for 5G communication systems. The proposed antenna achieves a resonant frequency of 3.75 GHz with excellent impedance matching, where the return loss reaches approximately -50 dB and the VSWR value is around 1.1, indicating efficient power transfer.

The design is further extended to a 4 × 4 MIMO configuration to enhance channel capacity and system reliability. Key MIMO performance parameters such as Envelope Correlation Coefficient (ECC), Mean Effective Gain (MEG), Total Active Reflection Coefficient (TARC), and Channel Capacity Loss (CCL) are analysed. The ECC value remains below 0.03, indicating low correlation and excellent diversity performance. Additionally, the CCL remains within acceptable limits, confirming minimal capacity loss.

Therefore, due to its compact size, wide bandwidth, good impedance matching, and strong MIMO performance, the proposed antenna is a suitable candidate for 5G, future 6G wireless systems, and Industry 5.0 communication applications.

7. REFERENCES

- [1] X. Wei High isolation MIMO antenna system for 5G N77/N78/N79 bands," *Micromachines*, vol. 15, no. 6, 721, 2024.
- [2] R.M. Asif, A.U. Rehman, S. Guizani, and H. Hamam, "Enhancing spectral efficiency in uplink/downlink channels of multi-cell massive MIMO for 5G networks," *International Journal of Advanced and Applied Sciences*, vol. 11, no. 8, pp. 66–79, 2024.
- [3] L. Chang, G. Zhang, and H. Wang, "Triple-band microstrip patch antenna and its four-antenna module based on half-mode patch for 5G 4 × 4 MIMO operation," *IEEE Transactions on Antennas and Propagation*, vol. 70, no. 1, pp. 67–74, Jan. 2022.

- [4] N. Anjum, Z. Yang, I. Khan, M. Kiran, F. Wu et al., "Efficient algorithms for cache-throughput analysis in cellular-d2d 5g networks," *Computers, Materials and Continua*, vol. 67, no. 2, pp.1759–1780, 2021.
- [5] T. Upadhyaya, I. Park, R. Pandey, U.Patel, K. Pandya, A. Desai, J.Pabari, G. Byun, and Y. Kosta, "Aperture-fed quad-port dual-band dielectric resonator-MIMO antenna for Sub-6 GHz 5G and WLAN application," *International Journal of Antennas and Propagation*, vol. 2022, pp. 1–13, Aug. 2022.
- [6] C. Z. Han, L. Xiao, Z. Chen, and T. Yuan, "Co-located self-neutralized handset antenna Pairs with complementary radiation patterns for 5G MIMO applications," *IEEE Access*, vol. 8, pp. 73151–73163, 2020.
- [7] W. Hu et al., "Wideband back-cover antenna design using dual characteristic modes with high isolation for 5G MIMO smartphone," *IEEE Transactions on Antennas and Propagation*, vol. 70, no. 7, pp. 5254–5265, July 2022.
- [8] A. J. A. A. Gburi et al., "Broadband circular polarised printed antennas for indoor wireless communication systems: A comprehensive review," *Micromachines*, vol. 13, no. 7, 1048, Jun. 2022.
- [9] X. Tian et al., "Power allocation scheme for maximizing spectral efficiency and energy efficiency tradeoff for uplink noma systems in B5G/6G," *Phys. Commun.*, vol. 43, 101227, Dec. 2020.
- [10] T. Y. Elganimi and K. M. Rabie, "Time-indexed parallel spatial modulation for large-scale MIMO systems with antenna grouping," in *Proc. of IEEE 93rd Vehicular Technology Conference (VTC2021-Spring)*, Helsinki, Finland, 2021, pp. 1–5.
- [11] R. Hussain, A. T. Alreshaid, S. K. Podilchak, and M. S. Sharawi, "Compact 4G MIMO antenna integrated with a 5G array for current and future mobile handsets," *IET Microw. Antennas Propag.*, vol. 11, no. 2, pp. 271–279, 2017.
- [12] M. Ahmed et al., "A blockchain-based emergency message transmission protocol for cooperative VANET," *IEEE Transactions on Intelligent Transportation Systems*, vol. 23, no. 10, pp. 19624–19633, Oct. 2022.
- [13] A. U. Makarfi, K. M. Rabie, O. Kaiwartya, O. S. Badarneh, X. Li, and R. Kharel, "Reconfigurable intelligent surface enabled IoT networks in generalized fading channels," in *Proc. of IEEE International Conference on Communications (ICC)*, Dublin, Ireland, 2020, pp. 1–6.
- [14] Y. Kabalci, "5G mobile communication systems: Fundamentals, challenges, and key technologies," in *Smart Grids and Their Communication Systems*, Berlin, Germany: Springer, Sep. 2019, pp. 329–359.
- [15] F. A. Ogaili and R. M. Shubair, "Millimeter-wave mobile communications for 5G: Challenges and opportunities," in *Proc. of IEEE International Symposium on Antennas and Propagation (APSURSI)*, Fajardo, PR, USA, 2016, pp. 1003–1004.
- [16] I. Rasheed, M. Asif, A. Ihsan, W. U. Khan, M. Ahmed, and K. M. Rabie, "LSTM-Based distributed conditional generative adversarial network for data-driven communications," *IEEE 5G-Enabled maritime UAV Transactions on Intelligent Transportation Systems*, Early Access, vol. 24, no. 2, pp. 2431–2446, 2022.
- [17] P. R. Girjashankar, T. Upadhyaya, and A. Desai, "Multiband hybrid MIMO DRA for Sub-6 GHz 5G and WiFi-6 applications," *International Journal of RF and Microwave Computer-Aided Engineering*, vol. 32, no. 12, pp. 1–18, Dec. 2022.
- [18] U. Patel and T. Upadhyaya, "Four-port dual-band multiple-input multiple-output dielectric resonator antenna for sub-6 GHz 5G communication applications," *Micromachines*, vol. 13, no. 11, pp. 1–17, Nov. 2022.
- [19] A. F. M. S. Shah, "A survey from 1G to 5G including the advent of 6G: Architectures, multiple access techniques, and emerging technologies," in *Proc. of IEEE 12th Annual Computing and Communication Workshop and Conference (CCWC)*, Las Vegas, NV, USA, 2022, pp. 1117–1123.
- [20] Y. Zhang, J. Du, Y. Chen, X. Li, K. M. Rabie, and R. Kharel, "Near optimal design for hybrid beamforming in mmWave massive multi user MIMO systems," *IEEE Access*, vol. 8, pp. 129153–129168, 2020.

- [21] M. B. Yassein, S. Aljawarneh, and A. A. Sadi, "Challenges and features of IoT communications in 5G networks," in Proc. of International Conference on Electrical and Computing Technologies and Applications (ICECTA), Ras Al Khaimah, United Arab Emirates, 2017, pp. 1–5.
- [22] A. Ahad, M. Tahir, M. Aman Sheikh, K. I. Ahmed, A. Mughees, and A. Numani, "Technologies trend towards 5G network for smart health-care using IoT: A review," *Sensors*, vol. 20, no. 14, 4047, Jul. 2020.
- [23] S. Talwar, D. Choudhury, K. Dimou, E. Aryafar, B. Bangerter and K. Stewart, "Enabling technologies and architectures for 5G wireless," in Proc. of IEEE MTT-S International Microwave Symposium (IMS2014), Tampa, FL, USA, 2014, pp. 1–4.
- [24] B. M. Zerihun and Y. Wondie, "Massive MIMO for 5G cellular networks: Potential benefits and challenges," *Lecture Notes of the Institute for Computer Sciences, Social Informatics and Telecommunications Engineering*, pp. 219–227, 2018.
- [25] M. Han, J. Du, Y. Zhang, X. Li, K. M. Rabie and G. Nauryzbayev, "Efficient hybrid beamforming design in mmWave massive MU MIMO DF relay systems with the mixed-structure," *IEEE Access*, vol. 9, pp. 66141–66153, 2021.
- [26] G. Irene and A. Rajesh, "A dual-polarized UWB-MIMO antenna with IEEE 802.11ac band-notched characteristics using split-ring resonator," *J. Comput. Electron.*, vol. 17, no. 3, pp. 1090–1098, Sep. 2018.
- [27] A. Khoshniat, "A linearly and circularly polarized active integrated antenna," Utah State University, 2011.
- [28] S. Saxena, B. K. Kanaujia, S. Dwari, S. Kumar, H. C. Choi, and K. W. Kim, "Planar four-port dual circularly-polarized MIMO antenna for Sub-6 GHz band," *IEEE Access*, vol. 8, pp. 90779–90791, 2020.
- [29] T. Duong, N. T. B. Phuong, P. D. Son, and V. V. Yem, "Improving characteristics of 28/38 GHz MIMO antenna for 5G applications by using double-side EBG structure," *Journal of Communications*, vol. 14, pp. 1–8, 2019.
- [30] S. P. Dubazane, P. Kumar, and T. J. O. Afullo, "Metasurface superstrate-based MIMO patch antennas with reduced mutual coupling for 5G communications," *The Applied Computational Electromagnetics Society Journal (ACES)*, pp. 408–419, 2022.
- [31] T. Alam, M. Faruque, and M. Islam, "A double-negative metamaterial-inspired mobile wireless antenna for electromagnetic absorption reduction," *Materials*, vol. 8, no. 8, pp. 4817–4828, Jul. 2015.
- [32] M. Islam, F. Ashraf, T. Alam, N. Misran, and K. Mat, "A compact ultrawideband antenna based on hexagonal split-ring resonator for pH sensor application," *Sensors*, vol. 18, no. 9, 2959, Sep. 2018.
- [33] J. M. Benlliure, M. C. Fabr s, E. A. Daviu, and M. F. Bataller, "Sector unit-cell methodology for the design of sub-6 GHz 5G MIMO antennas," *IEEE Access*, vol. 10, pp. 100824–100836, 2022.
- [34] Z. Ji et al., "Low mutual coupling design for 5G MIMO antennas using multi-feed technology and its application on metal-rimmed mobile phones," *IEEE Access*, vol. 9, pp. 151023–151036, 2021.
- [35] S. Li, B. Fu, and W. Cao, "A miniaturized Hexagon-shaped UWB Antenna," in Proc. of IEEE 3rd International Conference on Electronic Information and Communication Technology (ICEICT), Shenzhen, China, 2020, pp. 184–187.
- [36] A. Azari, "A new super wideband fractal microstrip antenna," *IEEE Transactions on Antennas and Propagation*, vol. 59, no. 5, pp. 1724–1727, May 2011.
- [37] S. F. Jilani and A. Alomainy, "Millimetre-wave T-shaped MIMO antenna with defected ground structures for 5G cellular networks," *IET Microwaves, Antennas & Propagation*, vol. 12, no. 5, pp. 672–677, Apr. 2018.
- [38] Y. Zhang, J. Du, Y. Chen, X. Li, K. M. Rabie, and R. Kharel, "Dual-iterative hybrid beamforming design for millimeter-wave massive multi-user MIMO systems with sub-connected structure," *IEEE Transactions on Vehicular Technology*, vol. 69, no. 11, pp. 13482–13496, Nov. 2020.